NASA-TM-80325 19820025037

NASA

Technical Memorandum 80325

A Technique for Determining Daytime Atmospheric Nitric Oxide from Backscattered Ultraviolet Measurements

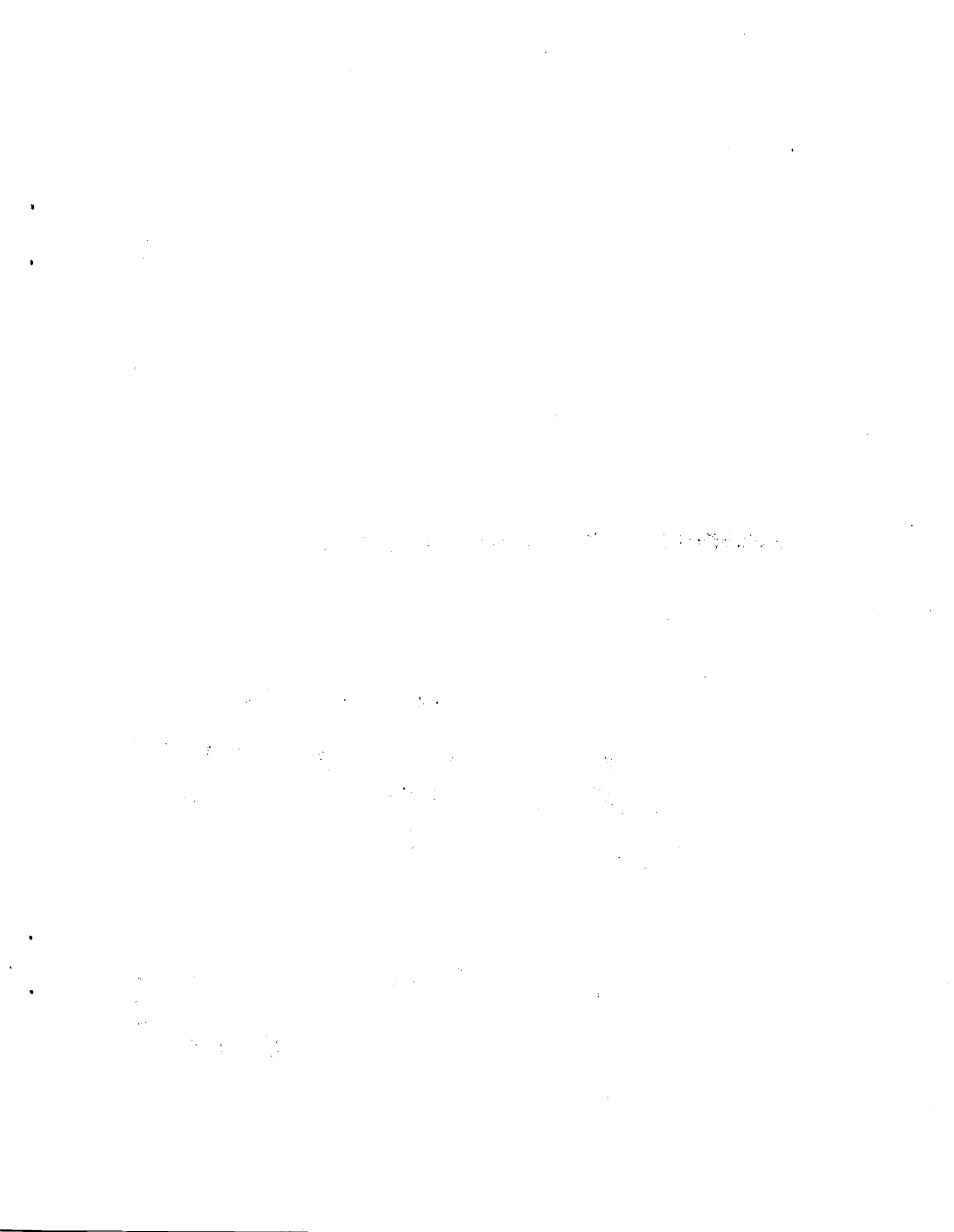B. Guenther, R. D. McPeters and J. E. Frederick

JULY 1979

National Aeronautics and
Space Administration

Goddard Space Flight Center
Greenbelt, Maryland 20771

A TECHNIQUE FOR DETERMINING DAYTIME ATMOSPHERIC NITRIC OXIDE FROM BACKSCATTERED ULTRAVIOLET MEASUREMENTS

B. Guenther

R. D. McPeters

J. E. Frederick
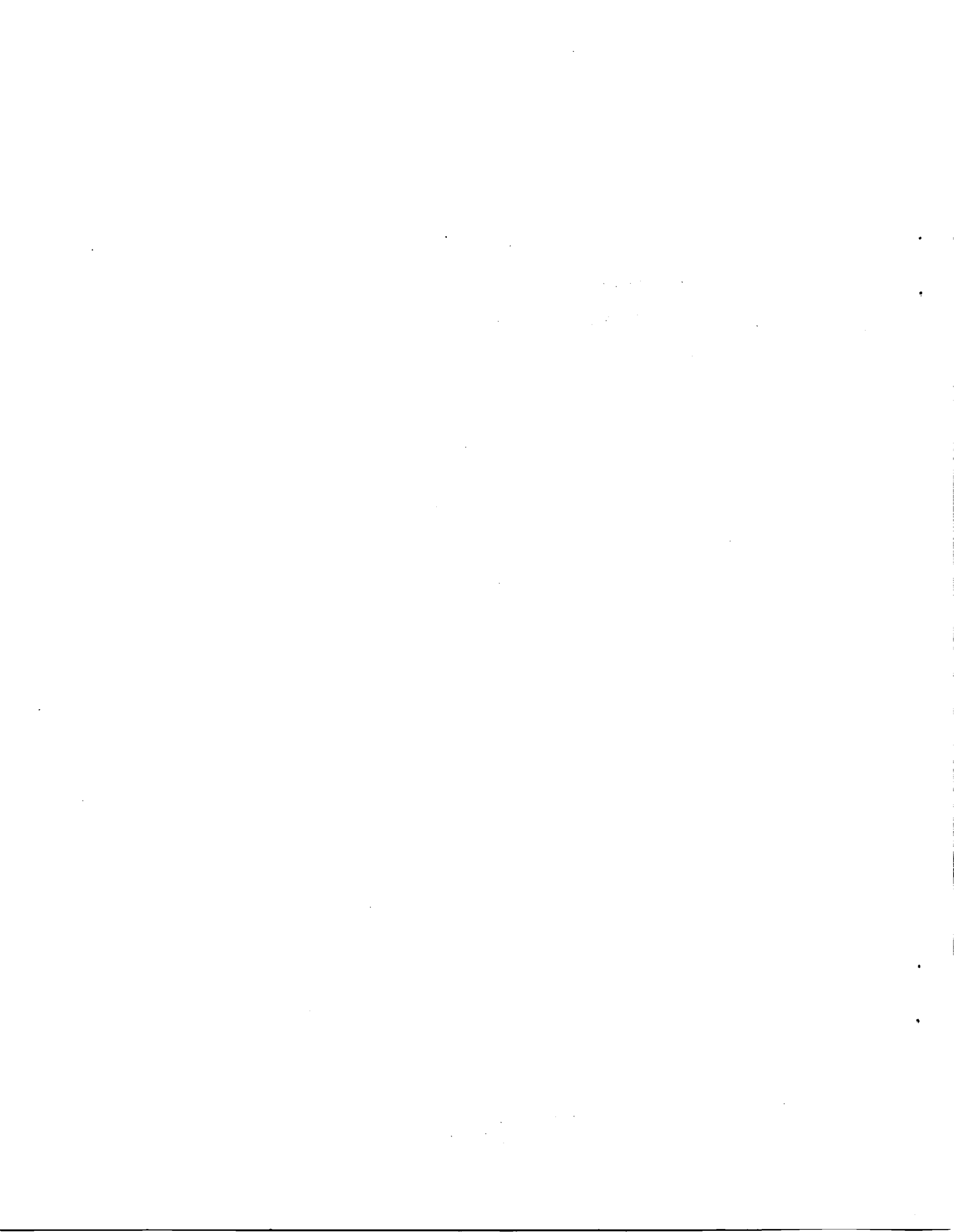
Laboratory for Planetary Atmospheres

Goddard Space Flight Center

Greenbelt, Maryland 20771

July 1979

N-153.220
N82-32913

A TECHNIQUE FOR DETERMINING DAYTIME ATMOSPHERIC NITRIC OXIDE CONTENT ABOVE 50 km FROM BACKSCATTERED ULTRAVIOLET MEASUREMENTS

B. Guenther

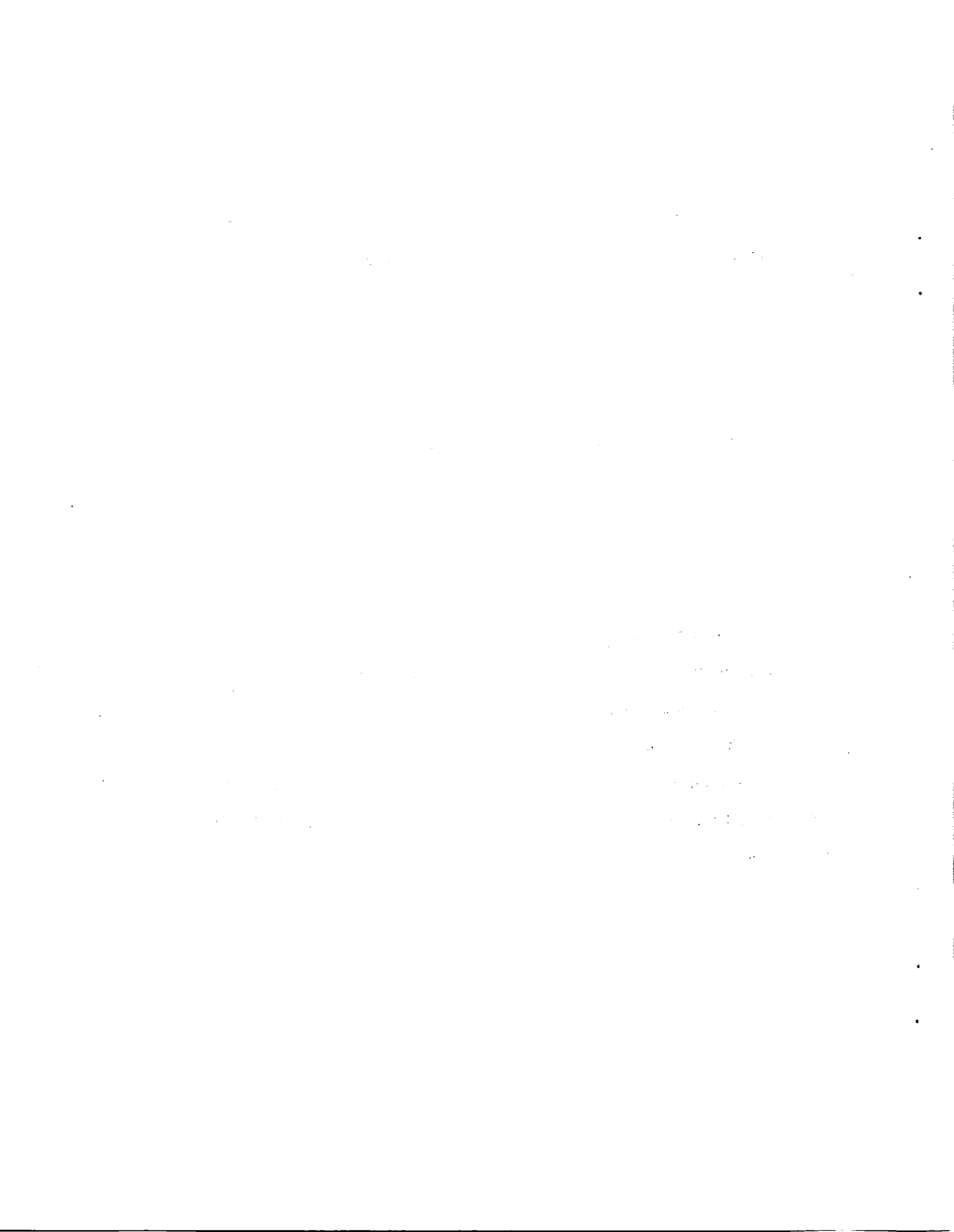R. D. McPeters

J. E. Frederick

Laboratory for Planetary Atmospheres

Goddard Space Flight Center
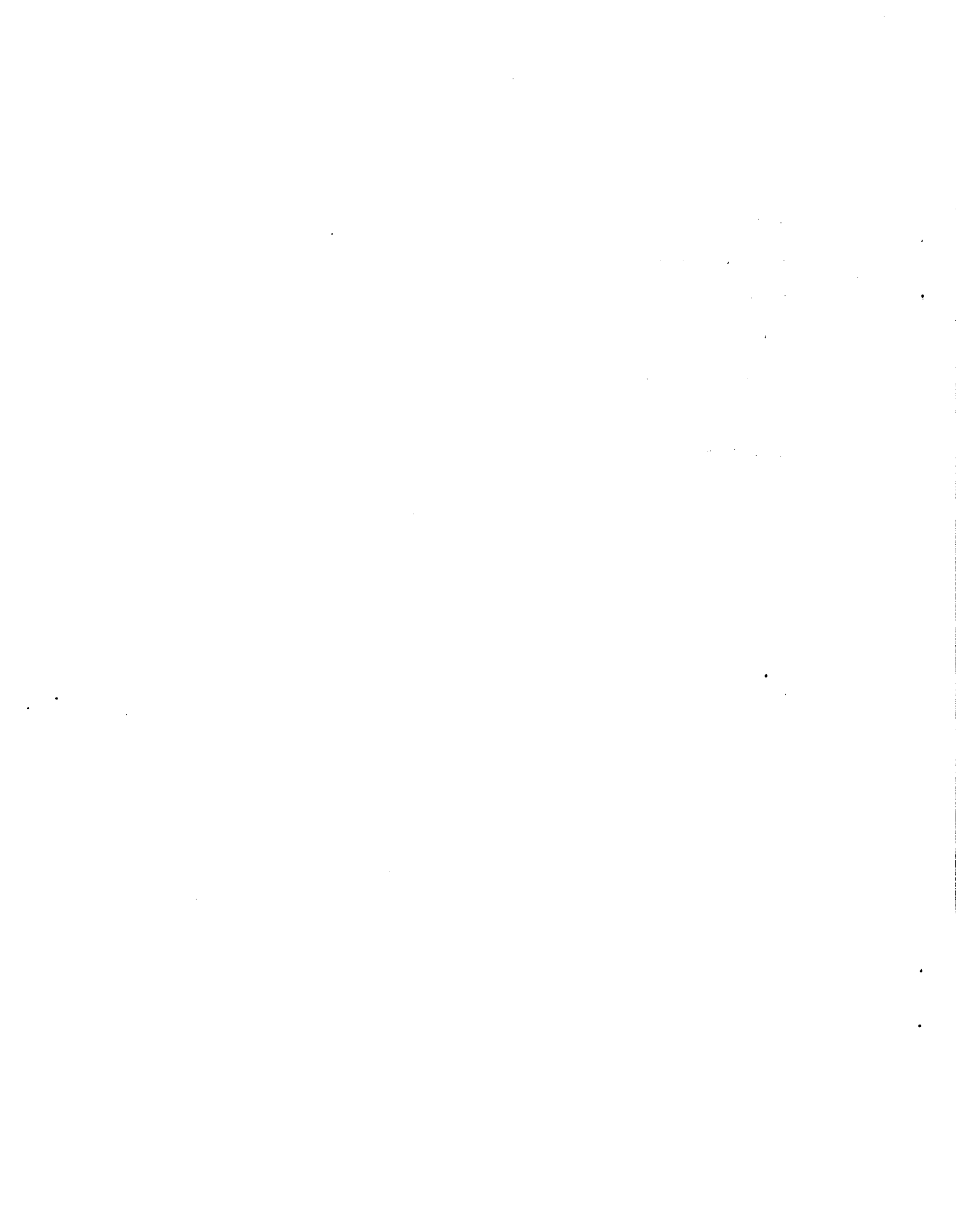
Greenbelt, Maryland 20771

ABSTRACT

Airglow from gamma band resonance fluorescence of nitric oxide near 255 nm is calculated at several solar zenith angles. Data from the Nimbus 4 BUV wavelengths 273.5 to 287.6 nm is used to estimate the rayleigh and ozone scattering contributions to the BUV 255.5 nm data and the remaining signal is attributed to NO airglow. The low solar zenith angle contributions by NO is less than 0.5%, and the high latitude/high zenith angle contribution exceeds 5%. This technique allows for estimating NO content above about 50 km, as well as partitioning that content between the mesosphere and thermosphere.

CONTENTS

A TECHNIQUE FOR DETERMINING DAYTIME ATMOSPHERIC
NITRIC OXIDE FROM BACKSCATTERED ULTRAVIOLET MEASUREMENTS

INTRODUCTION

Nitric oxide in the thermosphere and upper mesosphere has been investigated using both rocket and satellite measurements to study the D and E region ionosphere. NO in the lower mesosphere and stratosphere has received increased interest recently because it is active in catalytic destruction of ozone.

Measurements of NO in the middle atmosphere have been performed from balloon and rocket platforms.

Previous satellite studies of NO have measured airglow at 215 nm and interpreted the results in terms of NO gamma band resonance fluorescence. Difficulty in interpreting the rayleigh scattering contributions to the total 215 nm signal have limited these investigations to near terminator solar conditions for nadir observations and to observations in the thermosphere for horizon scanning observations. A new technique to observe nitric oxide related airglow is presented in this paper.

Accompanying NO gamma band 215 nm resonance fluorescence is radiation at 255.1 nm which is about 25% as intense as the 215 nm feature. Airglow at this wavelength is measured in the nadir by the Backscattered Ultraviolet (BUV) spectrometers in one of 8 discrete wavelength positions used for obtaining atmospheric ozone profiles. The amount of light expected at 255 nm from a pure ozone-rayleigh scattering atmosphere can be accurately determined from the remaining 7 BUV profiling wavelengths (273.5 to 305.8 nm), and the excess 255 nm radiation can then be interpreted in terms of nitric oxide resonance fluorescence. This technique provides a measurement of the NO content above 50 km for solar zenith angles above 30°.

BUV measurements (Heath et al., 1973) are available from two sun synchronous Nimbus satellites and a low inclination Atmosphere Explorer satellite. For the AE device which achieves a full

1

range of solar zenith angles in the latitude interval +20° to –20°, the excess 255.5 nm albedo is nearly constant at 5% and is attributed to an unknown solar zenith angle independent effect. For the Nimbus 4 and 7 measuring devices the minimum excess albedo is achieved at low solar zenith angles which coincide with low latitudes and amounts to about 5% of the measured values. For high solar zenith angles which are obtained at high latitudes the excess albedo scan has exceeded 15% in some instances.

The contribution to the BUV 255 nm data is calculated and shown to be inadequate to produce the mean 5% bias at low latitudes, but capable of explaining at least most of the latitude dependent 255.5 nm excess albedo observed with the Nimbus devices. A typical (mid-latitude) NO profile from 160 to 20 km is defined based on rocket measurements of NO and the airglow from resonance fluorescence for several solar zenith angles is calculated. A hypothetical latitude dependent NO contribution is then estimated based on satellite derived latitudinal variations in thermospheric NO and the resulting airglow is shown to be similar to the latitude variation in excess 255.5 nm albedo. A simple technique to determine the excess albedo from each BUV scan based on a Laplace Transformation inversion is used to provide a direct interpretation of the excess latitude dependent albedo in terms of NO content above 50 km. The computational model together with published thermospheric nitric oxide measurements for 1974 provide a way to identify separately the thermospheric and mesospheric amounts. The BUV shortest wavelength albedos interpreted in this way imply substantial latitude variability in mesospheric NO content with enhancements at 60° latitude and above up to a factor of 5 over typical mid-latitude content. Variations in mesospheric NO of this magnitude could have a significant impact on the ozone chemistry in the upper stratosphere where NO catalysis provides the major chemical sink for O_3.

The use of this technique on the Nimbus 4 and 7 BUV data base would provide a nearly complete measure of the NO content above 50 km from the earlier launch in April 1970 through the operating phase of Nimbus 7 which was launched in November 1978.

COMPUTATIONAL MODEL

Airglow at 255.1 nm can be produced by resonance fluorescence of nitric oxide in the gamma bands, where the primary feature is at 215 nm and the main secondary feature is at 255.1 nm. NO in the $X^2 II$ ($v = 0$) ground state is excited to the $A^2\Sigma^+$($v = 1$) state by absorption of a 215 nm photon. The primary deexcitation of the $v = 1$ state is fluorescence back to the ground state. For an optically thin atmosphere, this process has an emission rate factor $g_{v'v''}$, with $g_{10} = 7.69$ x 10^{-6} photons/molecule-s. The second brightest feature of the gamma bands is the transition to the $v = 4$ level of the $X^2\Pi$ state, yielding photons near 255.1 nm with an emission rate factor $g_{14} = 1.87$ x 10^{-6} photons/molecule-s (Barth, 1965). The 215 nm feature has been studied on several occasions, including rocket measurements (Barth, 1964) and two satellite measurements (see Rusch, 1973 and Stewart and Cravens, 1978). The 255.1 nm feature was also detected on the rocket measurement of Barth (1964) and the Ogo 4 measurement of Rusch (1973) but in neither case was this feature used to infer atmospheric NO content.

In this work, a model atmosphere including the neutral atmosphere, O_2, O_3 and NO has been constructed and used to estimate the contamination to 255.5 nm albedo by NO resonance fluorescence as a function of solar zenith angle. These calculations are also used to define the atmospheric NO content for a set of Nimbus 4 derived excess albedo values for the week 7–13 August 1970.

Figure 1 summarizes this model. The total optical depth, the optical depth for absorption from nitric oxide, molecular oxygen and ozone as well as Rayleigh scattering from the neutral atmosphere are shown as a function of altitude for 0° solar zenith angle. The neutral atmosphere is from the U.S. Standard Atmosphere, 1976 with a rayleigh scattering coefficient of 2.48 x 10^{-25} cm^2 molecule^{-1} at 215 nm (Allen, 1955). The ozone profile is the Krueger–Minzner Mid–Latitude Model (Krueger and Minzner, 1976) and the effective absorption coefficient at 215 nm was taken to be 1.0 x 10^{-18} cm^2 molecule^{-1} (Ackerman, 1971). A value of 9.4 x 10^{-18} cm^2 molecule^{-1} was adopted for the absorption coefficient at 255 nm (Inn and Tanaka, 1953). O_2 here was assumed to comprise a uniform 20% of the atmosphere with an effective absorption coefficient at 215 nm

3

of 7.94×10^{-24} cm^2 molecule^{-1} (Ackerman, 1971). The nitric oxide altitude distribution is shown in Figure 2 as the solid curve. The model shows a peak of 5×10^7 cm^{-3} at 105 km and a sharp minimum in concentration of 8×10^6 cm^{-3} at 85 km (adopted from Meira, 1971). The nitric oxide concentration in the lower mesosphere is adopted from Horvath and Mason (1979), and the profiles are made to be continuous between 70 and 60 km.

This model atmosphere is being used for calculating an integrated photon flux scattered to the top of the atmosphere and discontinuities in the first derivative of model NO profiles will have no effect on the results of this study. The X's in the figure show the profile between 70 and 20 km from McElroy et al., (1974) and are provided for comparison purposes. Two additional NO profiles above 70 km are shown as broken lines. These profiles are for NO peak concentrations of 1×10^7 and 8×10^7 cm^{-3} at 105 km, with all other values above 70 km scaled linearly from the 5×10^7 cm^{-3} (105 km) profile. The range of 1 to 8×10^7 cm^{-3} at the NO peak covers the typical zonal mean concentration reported from satellite observations in 1974 (Stewart and Cravens, 1978 and Cravens and Stewart, 1978). The emission rate factor adopted here is an effective value for the 1–4 transition of the gamma band. The 1–0 transition of the gamma band has been calculated in detail by Pearce (1969). That calculation shows that the transition is comprised of many rotational lines, with the absorption cross-section at the center of several of the rotational lines 50 to 100 times greater than the effective cross-section. For solar zenith angles up to about 75°, with modest path lengths through the atmosphere, the slant NO optical depth will be sufficiently small so that the effective emission rates of g_{10} and g_{14} will hold. For higher solar zenith angles the optical depth at the peak of the various rotational lines will become large and the flux transmitted will be differentially depleted at the center of the rotational lines. For these cases the effective emission rates g_{10} and g_{14} will decrease with altitude. Transmission by the atmosphere at 215 nm has been separated from $g_{v'v''}$ for small optical depths of NO in this calculation.

Equations 1 and 2 define the amount of light scattered to the top of the atmosphere by NO through resonance fluorescence.

$$L_{NO}(\lambda) = \int_0^\infty \epsilon(z,\lambda)dz = \sum_{n=1}^{51} \epsilon_n(\lambda) \tag{1}$$

where

L_{NO} is in units of ergs/cm^2-s-str,

$\epsilon(z,\lambda)$ is the differential contribution function for resonance fluorescence emitted at wavelength λ,

$\epsilon_n(\lambda)$ is the contribution function for the n-th layer emitted at wavelength λ.

$$\epsilon_n(\lambda) = \frac{1}{4\pi} N_n(NO) \cdot [g_{v'v''} \cdot T_z(\theta, 215\,nm)] \cdot T_z(0,\lambda) = \hat{\epsilon}_n(\lambda) \, T_z(0,\lambda) \tag{2}$$

and

$\hat{\epsilon}_n(\lambda)$ is the emission rate from layer n,

$T_z(0,\lambda)$ is the transmission by the atmosphere in the vertical above the altitude z for the n-th layer at wavelength λ,

$N_n(NO)$ is the vertical content of NO molecules in the n-th layer,

$g_{v'v''} = g_{10}$ for $\lambda = 215$ nm and g_{14} for $\lambda = 255.1$ nm,

$T_z(\theta, 215\,nm)$ is the transmission of incoming light to layer n at altitude z for a solar zenith angle θ at 215 nm which excites the NO molecule to the $A^2\Sigma^+(v=1)$ state.

These equations are for single scattering and observation of the radiation in the nadir from the top of the atmosphere. Computationally $T_z(0, 215)$ is relatively unimportant for $z \geqslant 50$ km, the altitude at which ozone absorption becomes the prime atmospheric attenuation process, and is increasingly under the control of O_3 absorption below this altitude. $T_z(0, 255.1)$ becomes important near 60 km and also is due exclusively to ozone absorption. The calculations were performed to near 40 km and the atmosphere was divided into 51 layers. Layer 1 is comprised of the atmosphere above 70 km, and all other layers are 2 km thick, extending from 70 to 20 km.

Figures 3 (a–d) show the 255.1 nm contribution function at solar zenith angles of 0, 60°, 70.5° and 78.5° respectively for each of the layers as well as the integrated amount of light reaching the top of the atmosphere originating at or above each layer at 255.1 and 215 nm for

the model atmosphere defined in Figure 1. The values for each layer are plotted at the bottom of the layer. Below 40 km ozone becomes highly absorbing at 255.1 nm and although 215 nm light has appreciable penetration to this altitude the airglow at 255 nm is absorbed within 1 ozone scale height of where it is emitted.

Detailed computations for several solar zenith angles are included as simple computational aids for extrapolating from this model atmosphere to an atmosphere with a different concentration at the 105 km peak. In all cases in this model for NO invariant at 60 km the contribution function at and below 60 km is a function only of the solar zenith angle (due to attenuation in the $T(\theta, 215)$ term); the 255.1 nm flux originating between 70 and 60 km represents about 4% of the total NO flux contribution and can be easily scaled (Figure 2) to the concentration at 60 and 70 km.

Figure 4 shows the solar zenith angle dependence of this resonance fluorescence mechanism for 0° to 80°. Above 80° g should be replaced by g(z). The open circles are the photon fluxes for 215 nm and must be referred to the left ordinate scale. The right side ordinate scale is the radiance at 255.7 nm which is implied by the 255.1 nm photon flux when detected by an instrument with a 1 nm triangular slit function with the centroid of the instrument bandpass 0.6 nm longer in wavelength than the 255.1 nm radiation — this describes the "255.5 nm" channel of the Nimbus 4 Backscattered Ultraviolet (BUV) Spectrometer. The X's in this Figure show the measured 255.7 nm radiation at several solar zenith angles from the Nimbus 4 BUV for a typical orbit, in this case 2 August 1972. This figure clearly shows that the radiation from this model atmosphere with the same NO profile at all latitudes is less than 1% of the total 255.5 nm radiation at low solar angles, and that the percent contribution from NO to the total radiation increases with increasing solar angle. The actual solar zenith angle dependence of the percent contribution of NO signal to the total BUV measurements is stronger than implied in this Figure; Cravens and Stewart (1978) have shown that the typical 105 km NO peak concentration is near $1 \times 10^7 \, cm^{-3}$ at low latitudes and $8 \times 10^7 \, cm^{-3}$ at high latitudes. Since the Nimbus 4 satellite is sun synchronous with a near

local noon equator crossing, we can relate low solar angles to low latitudes and high solar angles to high latitudes. For an NO latitude distribution where the thermospheric content varies as observed by Cravens and Stewart (1978), with a minimum at 0° solar zenith angle and a maximum at 70° the NO airglow contamination will grow from 0.3% to 5%.

DATA ANALYSIS

The computation has been reversed and the entire latitude dependent excess albedo has been interpreted as resonance fluorescence from NO for the Nimbus 4 data from 7–13 August 1970. A Laplace transform inversion has been applied to this data using the 273.5, 283.0 and 287.6 nm measurements to determine the ozone altitude profile in the region of the atmosphere where multiple scattering is unimprotant. The constraint for this inversion is that near the stratopause the ozone overburden above a pressure level p can be described as

$$X_p = Cp^{1/\sigma} \tag{3}$$

where σ is the ratio of the ozone scale height to the atmospheric scale height and C is the cumulative ozone above one millibar. Initial application of this technique to study BUV albedos was performed by Mateer (1972) and is currently used by McPeters (1979). By defining the quantities

$$Q = \frac{I(\lambda,\theta)}{E_0(\lambda)} \frac{4\pi}{S_{11}\beta\lambda}$$

and $\kappa = \alpha_\lambda(1 + ch(\theta))$

where $E_0(\lambda)$ is the extraterrestrial solar irradiance

$I(\lambda,\theta)$ Nadir radiance

θ Solar zenith angle

S_{11} Rayleigh scattering phase functions 3/4 $(1 + \cos^2\theta)$

β_λ Rayleigh volume atmosphere scattering coefficient (atm)$^{-1}$

α_λ Ozone absorption coefficient (atm. cm)$^{-1}$

$ch(\theta)$ Chapman function

the albedo for the four shortest wavelengths should lie on a straight line when $\ell n\ Q$ is plotted against $\ell n\ \kappa$. The $\ell n\ Q$s for 273.5 to 283.6nm do indeed fall on a straight line to high accuracy for all latitudes and seasons for the threeBUV sensors, and $\ell n\ Q255.5$ is systematically about 5% high at low latitudes and frequently more than 10% high at high latitudes. The excess 255.5nm albedo can be measured for each scan directly from $\ell n\ Q - \ell n\ \kappa$ plots. Figure 5 shows the mean logarithms of the deviation of the excess albedo with a 5% mean bias at all latitudes removed linearly. This is an estimate of the possible contribution of nitric oxide resonance fluorescence to this data set, and shows the standard behavior of increasing excess albedo with increasing solar zenith angle seen in the Nimbus data sets. The data are grouped in 10° latitude bins (top) or 10° solar zenith angle bins (bottom).

The excess albedo as shown in Figure 5 has been interpreted in terms of resonance fluorescence of nitric oxide in the thermosphere and mesosphere. In converting from measured albedo to implied radiance values we have used a solar flux of $70.2 \, ergs/cm^2\text{--}s\text{--}nm$ which is the preliminary Nimbus 7 255.5 nm result. We have attributed the maximum variability to NO in the thermosphere, consistent with Cravens and Stewart (1978), allowing for the 105 nm NO peak to vary between 1 and about $10 \times 10^7 \, cm^{-3}$. In the case of medium solar zenith angles the excess radiation was too large to be accounted for with the NO variation in the thermosphere alone, and it is necessary to provide substantially more NO in the mesosphere than is included in the model. The indication is that high thermospheric nitric oxide amounts are frequently accompanied by substantial enhancements in the mesospheric nitric oxide, and probably that the deep concentration minimum usually observed near 85km would be at least partially filled in by the downward transport of NO into the mesosphere. The NO values presented here are accurate to about a factor of 10, and the point-to-point precision is better than a factor of 2.

CONCLUSIONS AND DISCUSSION

Resonance fluorescence from nitric oxide in the mesosphere and thermosphere is shown to provide a significant latitude varying contribution to the measured Nimbus BUV signal at

255.5 nm. NO content above 50 km, as well as concentrations at 105 and 60 km can be estimated from measured BUV excess 255.5 nm albedo with appropriate assumptions about the latitude independent mean bias observed with the 3 BUV satellite sensors. The NO mesospheric content is shown to increase 5 fold in this data set from middle latitudes to high latitudes presuming that all the excess albedo at high latitudes — normalized to 0 excess at low latitudes — is due to NO airglow and that the thermospheric content is no larger than measured by Cravens and Stewart (1978). Since the latitudes at which these high mesospheric NO occur coincide with latitudes of high thermospheric NO production, it is at least possible that in these circumstances the mesospheric NO down to the stratopause (where this measurement technique loses sensitivity) is dominated by NO production above 90 km, and further then that there would be significant variations in upper stratospheric NO due to high concentrations above 50 km. The 85 km deep concentration minimum in NO would be smoothed in cases where NO produced above 90 km dominates the entire mesosphere.

Alternatively high mesospheric NO amounts may be produced there directly by the same processes that make NO in the thermosphere at these latitudes. The possibility that high mesosphere NO values result from enhanced vertical transport from below the stratopause cannot be precluded, but is considered less likely due to the coincidence of the latitude of these enhancements with the latitude region in which NO is efficiently produced through ion–recombination processes.

Calculations of the albedo enhancement at middle to high latitudes beyond that observed at the low latitudes were performed by tuning the ozone absorption coefficient at 255.5 nm differentially from 273.5 to 287.6 nm absorption coefficients to bring $\ln Q255.5$ onto a straight line at low latitudes. This required a change of about 7% in α, which provided a linear 5% change in 255.5 nm albedos at all solar zenith angles. This assumption was performed for computational simplicity; however, if the mean bias indeed results from an error in the set of αs then this is probably due to a small error in wavelength determination for the ozone absorption coefficients used (Inn and Tanaka, 1953) in the region where the absorption is changing rapidly with wavelength.

The excess albedo is not thought to be related to high altitude aerosol distribution because these effects would produce enhanced albedos at all the shorter BUV wavelengths. The Nimbus 7 device has less than 1% polarization sensitivity so the effect is not related to polarization phenomenon. The NO content measurements reported here will be upper or lower limits if the low latitude effect producing excess albedo is actually atmospheric, and becomes less or more effective with increasing latitude. The AE results require such an effect to have little or no solar zenith angle dependence at low latitudes.

The mean low latitude excess albedo which we have suppressed for these calculations might also result from fluorescence from another atmospheric species. For example, several bands from the Schumann-Runge system of molecular oxygen absorb within each wavelength channel sampled by the BUV. Band heads for the 7-10, 10-11 and 14-12 vibrational transitions are within the 255.5 nm channel. An emission efficiency of approximatly 1%, 0.5% and 10% respectively for any of these transitions would produce 1% of the measured 255.5 nm signal at $0°$ solar zenith angle or 20% of the excess albedo bias. This estimate uses the emission rate factors for the Schumann-Runge bands from Barth (1964), and presumes that O_2 absorption is the major attenuation of the incoming flux so that unit optical depth is reached where the column content of O_2 is given by the reciprocal of the absorption cross section. The O_2 partial pressure dependent absorption cross section is taken from Park (1974).

ACKNOWLEDGMENTS

REFERENCES

Ackerman, M., Ultraviolet solar radiation related to mesospheric processes, in Mesospheric Models and Related Experiments, ed. G. Fiocco, D. Reidel Pub. Co., 149–159 (1971).

Allen, C. W., Astrophysical Quantities, Athlone Press, London (1963).

Barth, C. A., Rocket measurement of the nitric oxide dayglow, J. Geophys. Res., 69, 3301–3303 (1964).

Barth, C. A., Ultraviolet spectroscopy of planets, J. P. L. Tech. Report No. 32-822 (1965).

Cravens, T. E. and A. I. Stewart, Global morphology of nitric oxide in the lower E regions, J. Geophys. Res., 83, 2446–2452 (1978).

Heath, D. F., C. L. Mateer and A. J. Krueger, Nimbus 4 backscatter ultraviolet (BUV) experiment — two years' operation, Pure and Applied Geophys. 106–108, 1238–1253 (1973).

Horvath, J. J. and C. J. Mason, Nitric oxide mixing ratios near the stratopause measured by a rocket-borne chemiluminescent detector, Geophys. Res. Lett. 1023–1026, (1978).

Inn, E. C. Y. and Y. Tanaka, Ozone absorption coefficients in the visible and ultraviolet regions, J. Opt. Soc. Am., 43, 870–873 (1953).

Krueger, A. K. and R. Minzner, Summary of a mid-latitude ozone model, in U.S. Standard Atmosphere, 36–40 (1976).

Mateer, C. L., Review of some aspects of inferring the ozone profile by inversion of ultraviolet radiance measurements, NASA Technical Memorandum X-62, 150 Mathematics of Profile Inversion, Ames. Research Center, Moffett Field, CA (L. Colin, ed.) (1972).

McElroy, M. B., S. C. Wofsy, J. E. Penner and J. C. McConnell, Atmospheric ozone: possible impact of stratospheric aviation, J. Atmos. Sci., 31, 287–303 (1974).
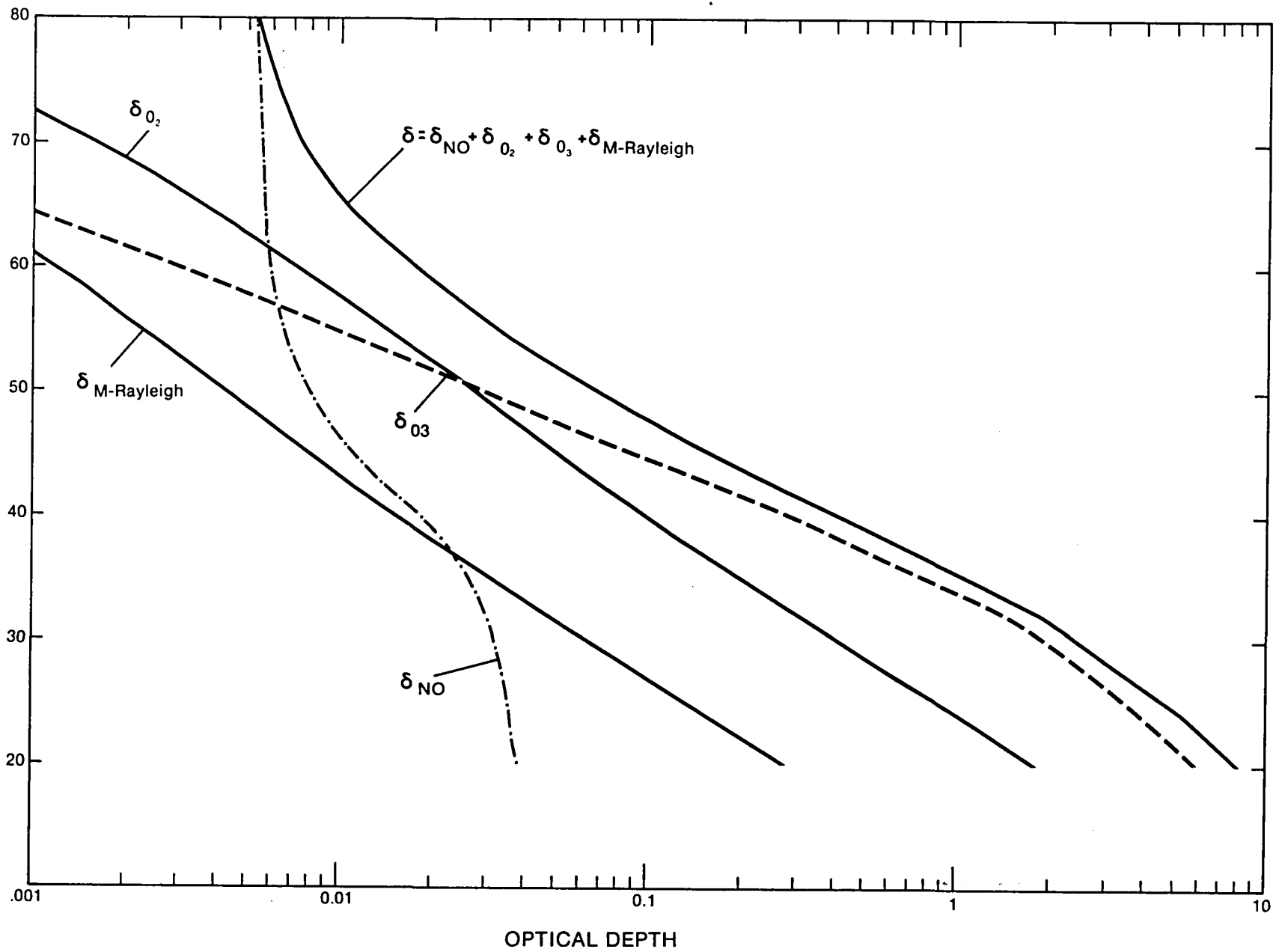
McPeters, R. D., Behavior of ozone near the stratopause from two years of BUV observations, submitted for publication (1979).

Meira, L. G., Jr., Rocket measurements of upper atmospheric nitric oxide and their consequences to the lower ionosphere, J. Geophys. Res., 76, 202–212, (1972).

Park, J. H., Equivalent mean absorption cross sections for the O_2 Schumann–Runge bands: application to the H_2O and NO photodissociation rates, J. Atmos. Sci., 31, 1893–1897 (1974).

Pearce, J. B., Nitric oxide gamma band emission rate factor, J. Quant. Spectrosc. Radiat. Transfer, 9, 1593–1602 (1969).

Rusch, D. W., Satellite ultraviolet measurements of nitric oxide fluorescence with a diffusive transport model, J. Geophys. Res., 78, 5676–5686 (1973).

Stewart, A. I. and T. E. Cravens, Diurnal and seasonal effects in E region low–latitude nitric oxide, 83, 2453–2456 (1978).

U.S. Standard Atmosphere, NOAA–S/T 76–1562, stock no. 003–017–00323–0, Superintendent of Documents, U.S. Government Printing Office, Washington (1976).
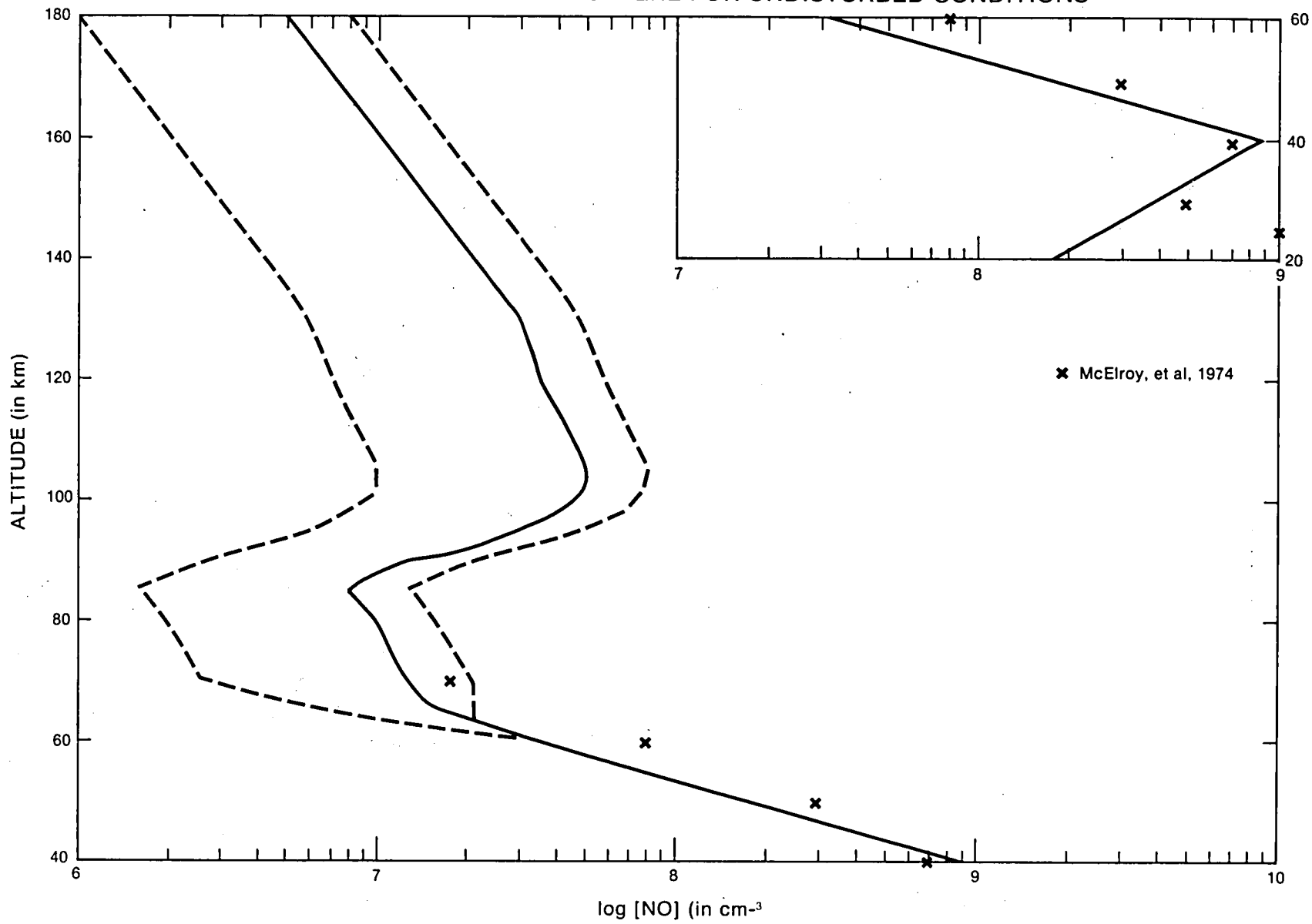
FIGURE CAPTIONS

Figure 1.   Optical depth as a function of altitude for solar flux at 215 nm for computational model using NO profile with 5×10^7 cm^{-3} at 105 km and 3.5×10^7 cm^{-3} at 60 km.

Figure 2.   Model nitric oxide atmosphere used in computations with NO 5×10^7 cm^{-3} at 105 km, as well as altitude distributions for thermospheric NO of 1 at 8×10^7 cm^{-3} at 105 km determined to be typical upper and lower limits by the AE UV Nitric Oxide experiment. For 5×10^7 cm^{-3} at 105 km, the NO content above 70 km is 2.42×10^{14} cm^{-2}.

Figure 3a. Contribution function for 2 km layers below 70 km for light at 255.1 nm, as well as the total integrated photon flux reaching the top of the atmosphere at 215 and 255.1 nm from altitudes down to each layer for 0° solar zenith angle for [NO] = 5×10^7 cm^{-3} at 105 km.

Figure 3b. Same as 3a, but for 60° solar zenith angle.

Figure 3c. Same as 3a, but for 70.5° solar zenith angle.

Figure 3d. Same as 3a, but for 78° solar zenith angle.

Figure 4.   Resonance Fluorescence from computational model for several solar zenith angles at 215 and 255.1 nm for [NO] = 5×10^7 cm^{-3} at 105 km, as well as measured Nimbus 4 BUV radiances measured on an orbit on 2 August 1972 plotted on the same scale as the 255.1 nm airglow.

Figure 5.   Latitude dependent component of the mean excess 255.5 nm albedo plotted as deviation from straight line for $\ln Q - \ln \kappa$ for Nimbus 4, 7–13 August 1970.

Figure 6.   NO concentration at 105 and 60 km and abundance above 50 km implied by latitude dependent mean excess 255.5 nm radiation for data from Figure 5.
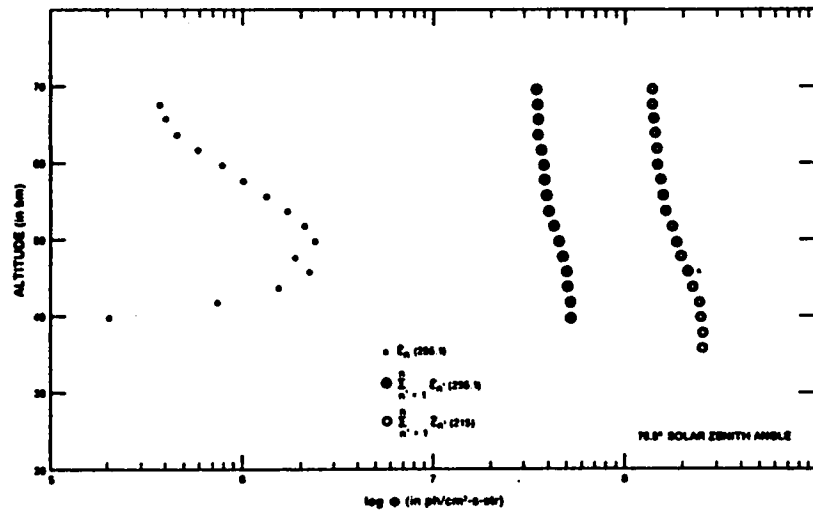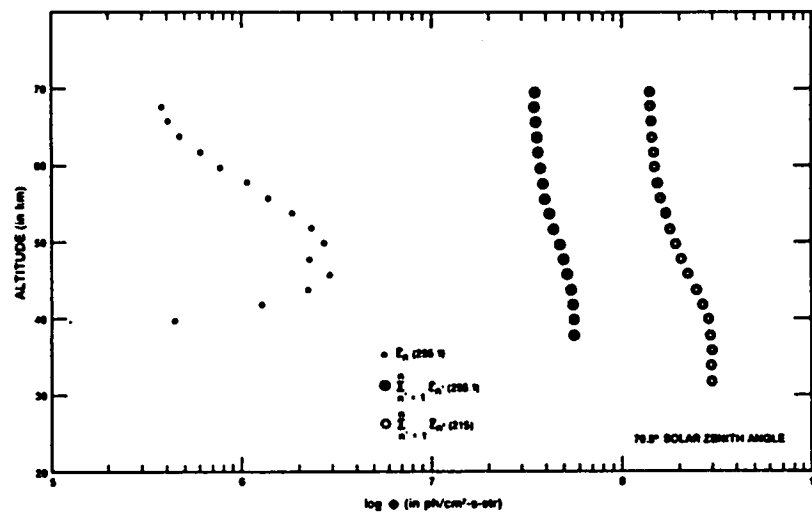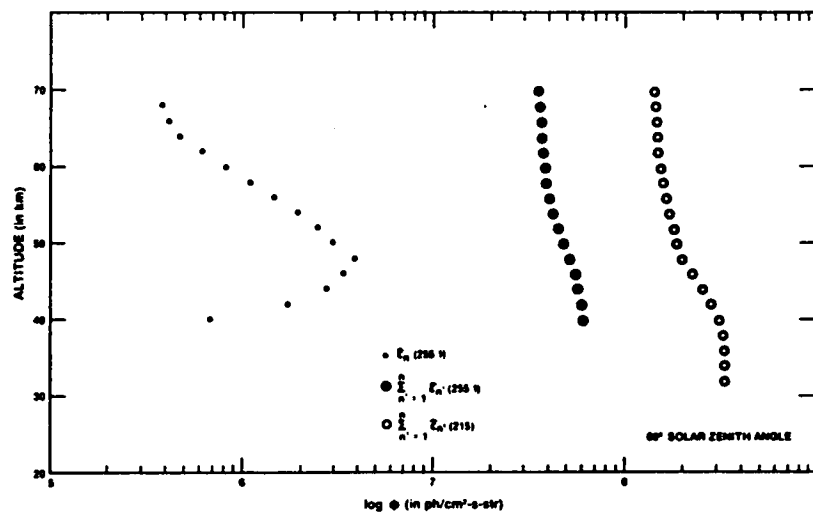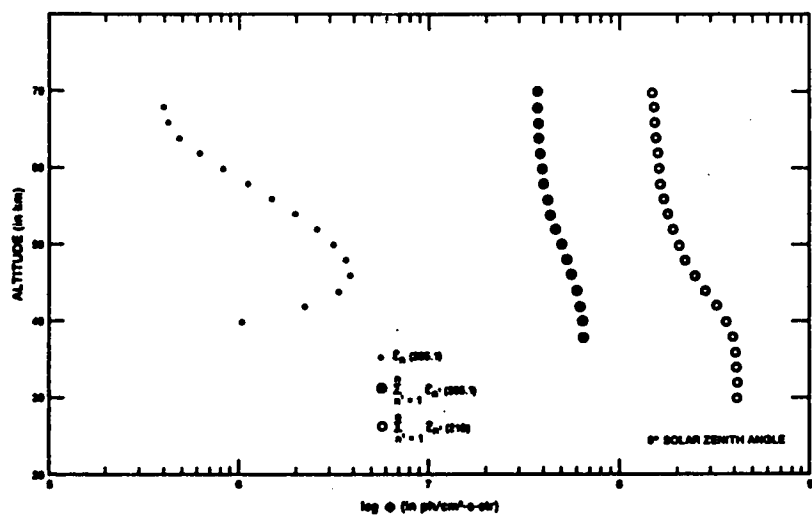
VERTICAL OPTICAL DEPTH AT 215.0 nm FOR MODEL ATMOSPHERE

δ_{O_2}
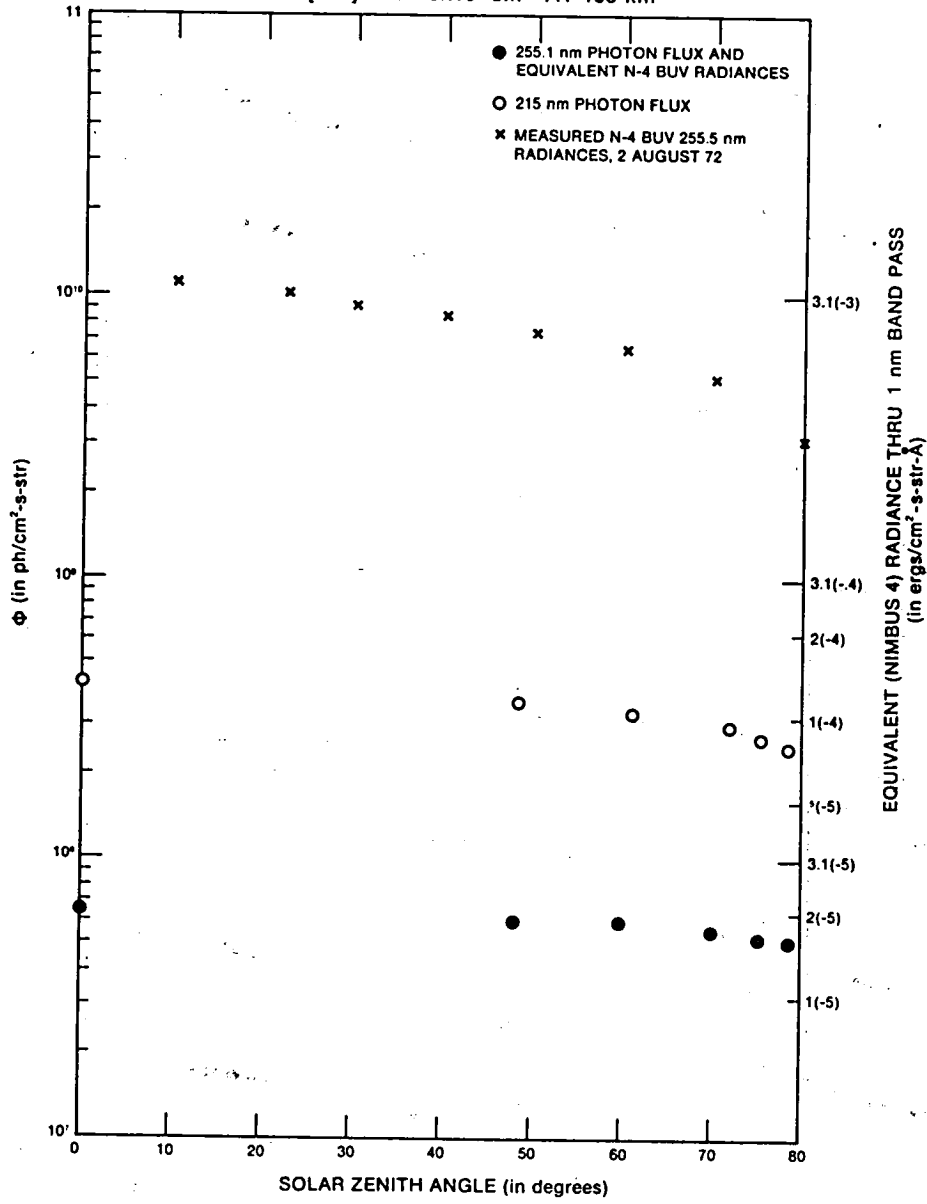
$\delta = \delta_{NO} + \delta_{O_2} + \delta_{O_3} + \delta_{M\text{-}Rayleigh}$

$\delta_{M\text{-}Rayleigh}$

δ_{O3}

δ_{NO}

OPTICAL DEPTH

BASIC NO MODEL ATMOSPHERE FOR UNDISTURBED CONDITIONS
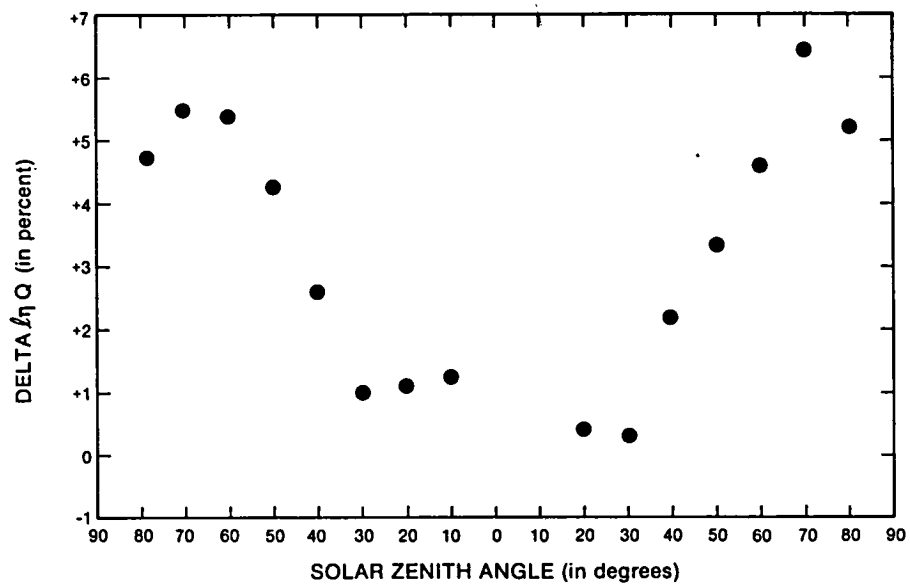
✖ McElroy, et al, 1974

ALTITUDE (in km)

log [NO] (in cm⁻³

BACKSCATTERED ULTRAVIOLET FROM MODEL NO ATMOSPHERE
WITH $[NO]max = 5 \times 10^7$ cm^{-3} AT 105 km

Legend:
- ● 255.1 nm PHOTON FLUX AND EQUIVALENT N-4 BUV RADIANCES
- ○ 215 nm PHOTON FLUX
- ✕ MEASURED N-4 BUV 255.5 nm RADIANCES, 2 AUGUST 72

Y-axis (left): Φ (in ph/cm^2-s-str)

Y-axis (right): EQUIVALENT (NIMBUS 4) RADIANCE THRU 1 nm BAND PASS (in ergs/cm^2-s-str-Å)
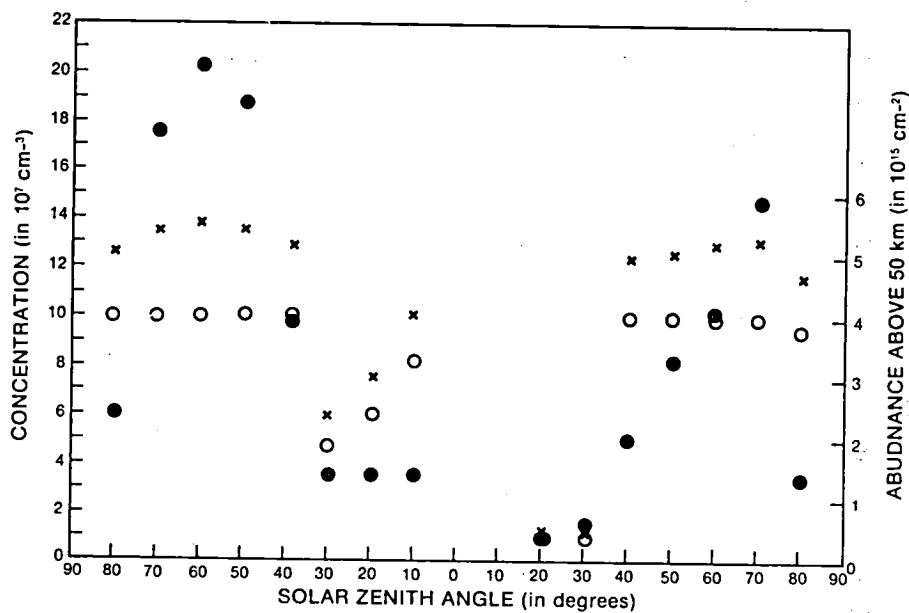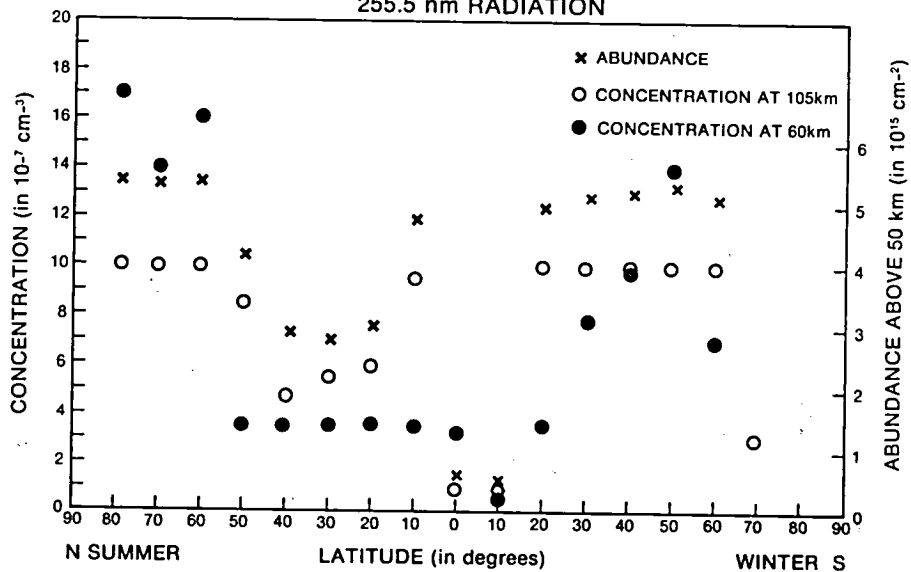
X-axis: SOLAR ZENITH ANGLE (in degrees)

MEANS EXCESS 255.5 nm ALBEDO
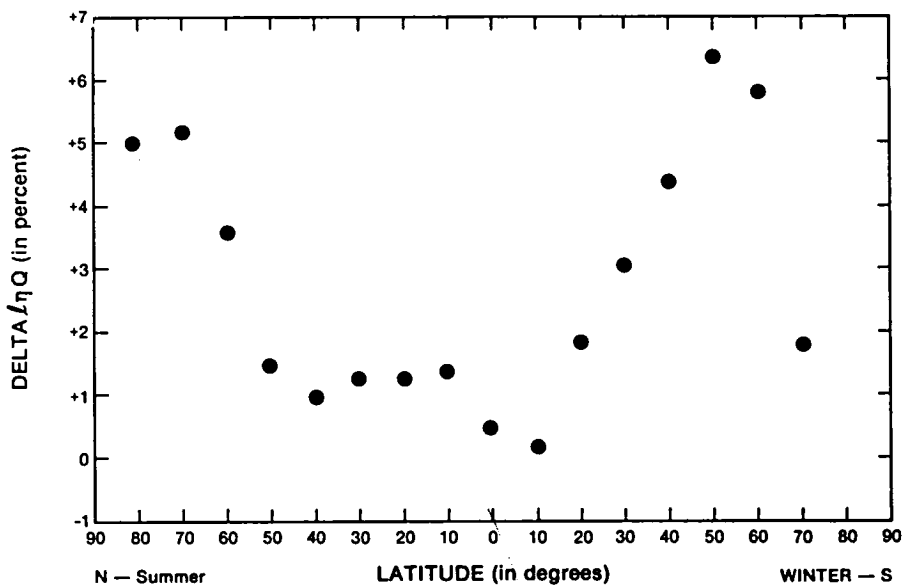
DATA FROM NIMBERS 4 BUV FOR
7-13 AUGUST 1970

NO CONCENTRATIONS AND ABUNDANCE ABOVE 50 km
IMPLIED BY MEAN EXCESS
255.5 nm RADIATION

DATA FROM NIMBUS 4 BUV FOR
7-13 AUGUST 1970

1. Report No. TM 80325	2. Government Accession No.	3. Recipient's Catalog No.
4. Title and Subtitle A Technique for Determining Daytime Atmospheric Nitric Oxide Above 50km From Backscattered Ultraviolet Measurements		5. Report Date
		6. Performing Organization Code 960
7. Author(s) B. Guenther, R. D. McPeters, J. E. Frederick		8. Performing Organization Report No.
9. Performing Organization Name and Address Laboratory for Planetary Atmospheres Goddard Space Flight Center Greenbelt, MD 20771		10. Work Unit No.
		11. Contract or Grant No.
		13. Type of Report and Period Covered
12. Sponsoring Agency Name and Address NASA Goddard Space Flight Center Greenbelt, MD 20771		TM
		14. Sponsoring Agency Code NASA

15. Supplementary Notes

16. Abstract

   Airglow from gamma band resonance fluorescence of nitric oxide near 255 nm is calculated at several solar zenith angles. Data from the Nimbus 4 BUV wavelenghts 273.5 to 287.6 nm is used to estimate the rayleigh and ozone scattering contributions to the BUV 255.5 nm data and the remaining signal is attributed to NO airglow. The low solar zenith angle contributions by NO is less than 0.5%, and the high latitude/high zenith angle contribution exceeds 5%. This technique allows for estimating No content above about 50 km, as well as partitioning that content between the mesosphere and thermopshere.

17. Key Words (Selected by Author(s)) Nitric Oxide, Upper Atmosphere, Satellite Technique	18. Distribution Statement

19. Security Classif. (of this report)	20. Security Classif. (of this page)	21. No. of Pages	22. Price*